Optical metrology: Methodological analogy and duality revisited

Mitsuo Takeda*
Center for Optical Research and Education (CORE), Utsunomiya University
7-1-2, Yoto, Utsunomiya, Tochigi, 321-8585, Japan

ABSTRACT

Analogy and duality help systematic and unified understanding of the seemingly different principles of optical metrology. As an ode honoring Jim Wyant and his achievements in optical metrology, I would like to present a review that revisits the time-space analogy and signal-frequency duality in optical metrology.

Keywords: Optical metrology, analogy, duality, interferometry, coherence holography

1. INTRODUCTION

Recent advance in optical metrology has seen a wide variety of techniques that have been developed to meet different needs in applications[1]. Despite their apparent diversity, we can find methodological analogy and duality in their basic principles. Analogy and duality are not only of interest *per se* but they also provide new insights that help unified and systematic understanding of the seemingly different principles of optical metrology. I have been interested in this subject since 1997 when Fringe Conference was held in Bremen, Germany, where Program Chair, Wolfgang Osten, gave me a challenging talk title *The Philosophy of Fringe.* As my partial answer to his hard homework beyond my ability, I talked about my personal view on analogy and duality in optical metrology[2]. More than twenty years have passed since then, and new development has been made in the field. So, I would like to take this opportunity to revisit the subject for update and present a review talk as my tribute to Jim Wyant, honoring his achievements in optical metrology.

2. ORIGIN OF ANALOGY AND DUALITY

The wave equation for an optical field $\nabla^2 u(\boldsymbol{r},t) = (1/c^2)[\partial^2 u(\boldsymbol{r},t)/\partial t^2]$ has space-time symmetry in its mathematical form of second-order partial derivatives with respect to space and time variables $\boldsymbol{r}$ and t. Generally, optical fields used in optical metrology are composed of elementary plane waves

$$\exp[i(\boldsymbol{k}\cdot\boldsymbol{r}-\omega t)] = \exp(i\boldsymbol{k}\cdot\boldsymbol{r})\exp(-i\omega t) \ , \tag{1}$$

with $\boldsymbol{k}$ and ω being spatial and temporal angular frequencies, respectively. Note that the elementary planewave inherits

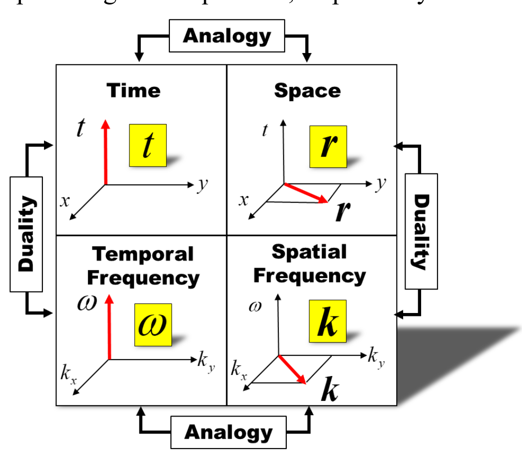

Figure 1. Space-time-analogy and signal-frequency-duality relations between the four variables $(t,\boldsymbol{r},\omega,\boldsymbol{k})$.

*takeda@opt.utsunomiya-u.ac.jp

Tribute to James C. Wyant: The Extraordinaire in Optical Metrology and Optics Education,
edited by Virendra N. Mahajan, Daewook Kim, Proc. of SPIE Vol. 11813, 118130J

the symmetry of the wave equation and have two-fold symmetries between the variables in space $(\boldsymbol{k},\boldsymbol{r})$ and time (ω,t), as well as between the variables in signal domain $(\boldsymbol{r},t)$ and frequency domain $(\boldsymbol{k},\omega)$. This formal symmetry permits interchanging the functional roles played by the variables (except the causality imposed on the time variable), and thereby serves as the origin of analogy and duality. The possible combinations of these four variables $(\boldsymbol{k},\boldsymbol{r};\omega,t)$ in the parameter space create a technological playground for researchers to play various games of optical metrology. Figure 1 summarizes the relations between these four variables in a diagram showing space-time analogy and signal-frequency duality. The space-time analogy suggests that, if there is a principle of optical metrology that works with a time variable, there is a similar principle that works with a space variable, and *vice versa*. Similarly, the duality between the signal domain and the frequency domain suggests that, if there is a principle of optical metrology that works in the signal domain, there is a similar principle that works in the frequency domain, and *vice versa*.

3. SPACE-TIME ANALOGY IN HETERODYNE INTERFEROMETRY

A well-known example is space-time analogy in heterodyne interferometry. In the temporal carrier technique, an object beam $A_O \exp[i(\boldsymbol{k}\cdot\boldsymbol{r}-\omega t+\phi(x,y))]$ is superposed on a reference beam $A_R \exp[i(\boldsymbol{k}\cdot\boldsymbol{r}-(\omega+\Delta\omega)t)]$ with the frequency slightly shifted by a frequency shifter (e.g., an acousto-optic modulator), as shown in Fig. 2 (top). Through interference, a temporal carrier fringe signal $g(x,y;t)$ is generated, with a carrier frequency $2\pi f_0 t=\Delta\omega t$ resulting from temporal frequency beating, which permits electronical detection of the optical phase information $\phi(x,y)$ [3]. The phase shift technique[4] may be regarded as a variant of the temporal carrier technique in which the temporal fringe is sampled at discrete intervals over one fringe period. This can be done by a stepwise movement of a reference mirror with a piezo-electric transducer, and the phase is detected by the phase shift algorithm.

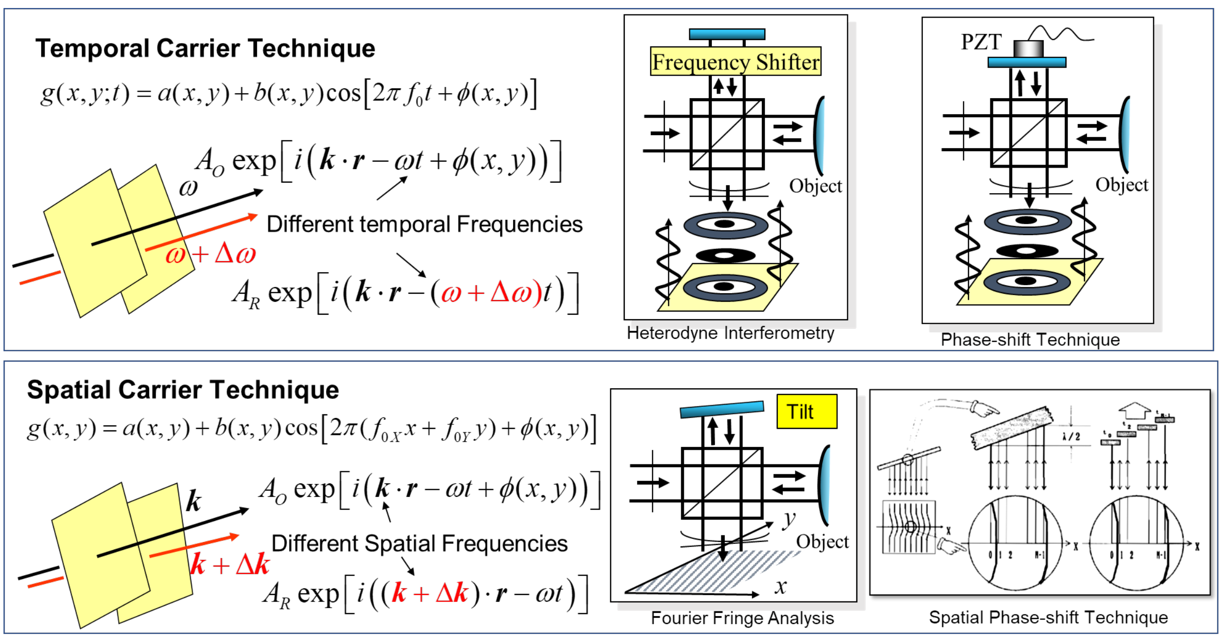

Figure 2. Space-time analogy in heterodyne interferometry.

Alternatively in the spatial carrier technique, the object beam $A_O \exp[i(\boldsymbol{k}\cdot\boldsymbol{r}-\omega t+\phi(x,y))]$ interferes with a reference beam $A_R \exp[i((\boldsymbol{k}+\Delta\boldsymbol{k})\cdot\boldsymbol{r}-\omega t)]$ with its spatial frequency (represented by a wavevector $\boldsymbol{k}$) slightly shifted by giving a small tilt to the wavefront, as shown in Fig. 2 (bottom). Through interference, a spatial carrier fringe pattern $g(x,y)$ is generated, with a spatial carrier frequency $2\pi(f_{0X}x+f_{0Y}y)=\Delta\boldsymbol{k}\cdot\boldsymbol{r}$ resulting from spatial frequency beating (or moiré), which permits the detection of the optical phase information $\phi(x,y)$ by the Fourier transform method[5] (known also as Fourier fringe analysis). A variant of spatial carrier technique is the spatial phase-shift technique shown in Fig. 2 (bottom right). If we take a closer look at one fringe period of the spatial carrier fringe pattern, and note that the tilted mirror is giving a spatial sequence of phase shits (just like a set of axially-shifted tiny discrete mirrors), then we can regard the one period of the spatial carrier fringe pattern as being a spatially encoded phase-shift fringe signal to which the phase-shift algorithm is applicable[6].

4. SPACE-TIME ANALOGY AND SPECTRAL FRINGES IN FILM-THICKNESS MEASUREMENTS

Let us compare four different principles of interferometric film-thickness measurements, and see space-time analogy that involves fringes in spectral domain. Shown in Fig. 3 (a) is a technique of white-light interferometry based on temporal signal-domain correlation[7], which may be regarded as the predecessor of the correlation domain OCT (optical coherence tomography). Collimated white light from a broadband point source is reflected from the top and bottom surfaces of a film with time delay Δt proportional to the film thickness d . The reflected lights do not interfere with each other because their temporal coherence is much shorter than the time delay, but they can be made to interfere with each other by compensating the delay with an interferometer that has a variable arm length. The film thickness is determined from

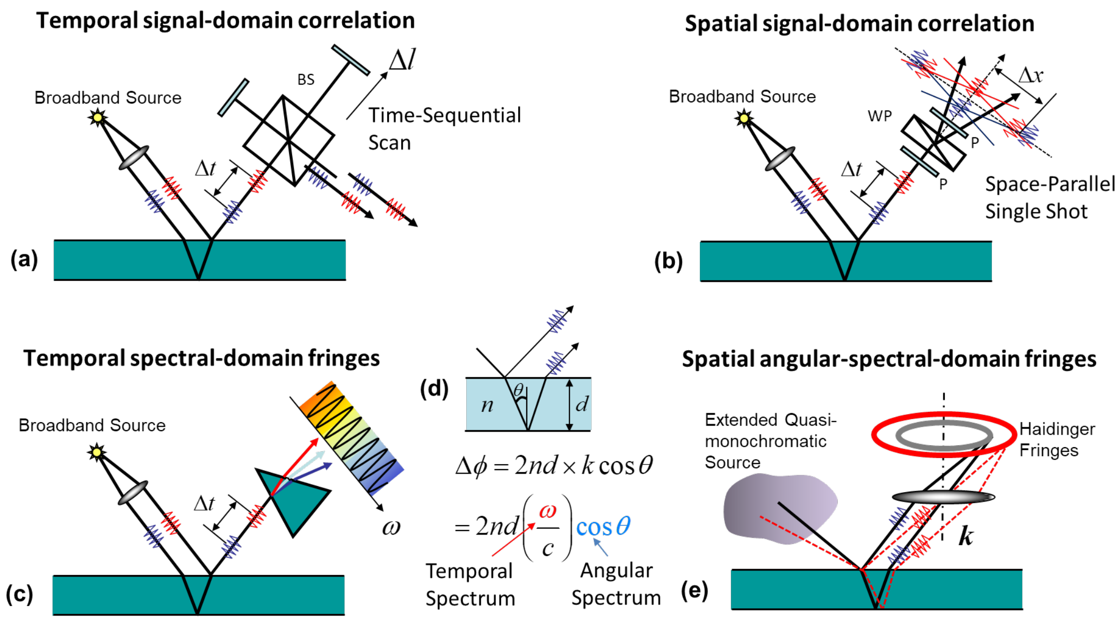

Figure 3. Principles of interferometric film-thickness measurements. (a) Temporal signal-domain correlation, (b) spatial signal-domain correlation, (c) temporal spectrum-domain fringes, (d) the relation of phase difference to temporal spectrum and angular spectrum, and (e) spatial angular-spectral-domain fringes

the amount of the time delay introduced by the interferometer to generate a white-light fringe. Figure 3 (b) shows white-light interferometry based on spatial signal-domain correlation[8]. Instead of the sequential mechanical scan of the interferometer arm for the time-delay compensation, the time delay Δt is introduced parallelly as a spatial distribution with Δx as a variable, for which use is made of a Wollaston prism that gives a tilt to the wavefronts. As with the case of spatial carrier heterodyne interferometry shown in Fig. 2 (bottom right), the wavefront tilt encodes the time delay into the spatial coordinate and permits a single shot measurement. Furthermore, signal-frequency duality permits yet another scheme of single-shot measurements in spectrum domains. Shown in Fig.3 (c) is a scheme based on the detection of temporal spectral fringes[9], which may be regarded as the predecessor of the spectral domain OCT. The white lights with mutual time delay are introduced into a spectrometer to observe their spectral fringes. The spectral fringes changes their brightness periodically with a period inversely proportional to the time delay Δt, alternating at the optical frequencies ω for which the phase difference $\Delta\phi$ introduced by the film thickness (see Fig. 3 (d)) is integer multiples of 2π. Therefore, by computing the Fourier transform of the spectral fringe, the film thickness can be determined from the position of the spectral peak. Shown in Fig. 3 (e) is an alternative scheme that detects spatial angular-spectral fringes in the spatial frequency domain. As shown in Fig. 3 (d), the phase difference $\Delta\phi$ introduced by the film thickness depends not only on the temporal frequency ω but also on the spatial angular frequency $k\cos\theta = (\omega / c)\cos\theta$. Instead of the white-light point source, we make use of a quasi-monochromatic spatially-incoherent extended source, which serves as a broadband angular-spectrum source that illuminates the sample with a wide range of angles. The spatial angular-spectral fringes (better known as Haidinger fringes) are observed at infinity in the focal plane of the Fourier transform lens[10]. Bause of the $k\cos\theta$ dependence of the phase difference, the fringes look like a part of a Fresnel zone plate, but the film thickness can be determined by fitting the fringe pattern with an appropriate fringe model. Because monochromatic light is used, the technique is free from the problem of refractive-index dispersion of the film caused by white light.

5. ANALOGY IN COHERENCE-BASED OPTICAL METROLOGY

5.1 Analogy between coherence theory and diffraction theory

The coherence function $\Gamma(\boldsymbol{r}_1,t_1;\boldsymbol{r}_2,t_2)=\langle u^*(\boldsymbol{r}_1,t_1)u(\boldsymbol{r}_2,t_2)\rangle$ and the optical field $u(\boldsymbol{r},t)$ obey the same wave equation[11]:

$$\begin{pmatrix}\text{Coherence}\\ \text{Function}\end{pmatrix}\quad \nabla^2_{i=1,2}\Gamma(\boldsymbol{r}_1,t_1;\boldsymbol{r}_2,t_2)=\frac{1}{c^2}\frac{\partial^2\Gamma(\boldsymbol{r}_1,t_1;\boldsymbol{r}_2,t_2)}{\partial t^2_{i=1,2}};\qquad \begin{pmatrix}\text{Optical}\\ \text{Field}\end{pmatrix}\quad \nabla^2 u(\boldsymbol{r},t)=\frac{1}{c^2}\frac{\partial^2 u(\boldsymbol{r},t)}{\partial t^2} \tag{2}$$

As a natural consequence of this fact, one may note a formal similarity between the diffraction integral and the formula of van Cittert-Zernike theorem[12]. For example, the Fraunhofer diffraction from a coherently illuminated circular aperture results in a familiar Airy pattern of the form $u(r)\propto 2J_1(\alpha r)/\alpha r$ (α being an appropriate scale factor). If the aperture is illuminated by spatially incoherent light, the Airy pattern will be replaced by a nearly uniform intensity distribution without structure. Nonetheless, by using an appropriate interferometer for field correlation, we can detect the coherence function that has exactly the same form $\Gamma(\Delta r)\propto 2J_1(\alpha\Delta r)/\alpha\Delta r$, with Δr being the separation between two points on the observation plane. This analogy between coherence theory and diffraction theory leads to the concept of coherence holography[13], in which a recorded 3-D object is reconstructed by the distribution of a coherence function, rather than by the optical field distribution as in conventional holography.

5.2 Coherence holography and coherence synthesis

Here we explain the principle of coherence holography intuitively from the view point of the reciprocity in holographic recording and reconstruction[14], so that we can exclude the mathematics used in the original paper[13]. Referring to Fig.4 (a), we first consider recording of a conventional hologram with coherent illumination. Just for simplicity of the explanation, we consider the case in which a point object at P is recorded with a reference beam from a point source at R. If the hologram is recorded in a plane normal to the optical axis PR (defined by the line connecting the object and the reference source), we have an on-axis (Gabor-type) hologram with a FZP (Fresnel zone plate) fringe pattern. On the other hand, if the hologram is recorded in a plane parallel to the optical axis PR, we have an off-axis (Leith-type) hologram with a Young's straight fringe pattern. In either case, the bright fringe is created at every point S on the hologram for which the OPD (optical path difference) between the object and reference beams (PS-RS) makes the two beams in phase at point S. If the hologram is illuminated from backward with a phase-conjugated reference spherical beam converging into point R, the point object is reconstructed at its original point P by a spherical beam converging into point P. A spurious twin

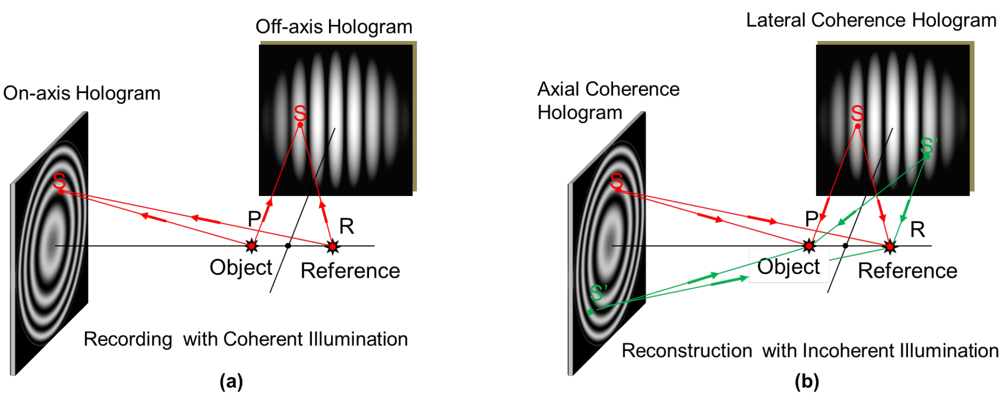

Figure 4. Reciprocity in holographic recording and reconstruction. (a) Holographic recording with coherent illumination. (b) Holographic reconstruction with spatially incoherent illumination.

image (called conjugate image) is also reconstructed on the optical axis at point P' (not shown) in symmetry to R, but we ignore it, for simplicity, regarding it as an unwanted noise image, as in most cases of conventional holography. Thus, for coherent illumination, the on-axis hologram functions as a lens that focuses the optical field into the axially shifted point P, while the off-axis hologram functions as a prism that tilts the optical field to converge into the laterally shifted point P. Strictly speaking, they function as a bifocal lens and a biprism, respectively, if we take the ignored twin image into consideration. So much for conventional holography, and we next explain the principle of coherence holography.

Referring to Fig. 4 (b), let us now illuminate the holograms from backward with quasi-monochromatic spatially incoherent light (or let the holograms be quasi-monochromatic self-illuminating extended spatially-incoherent sources). The optical field is focused at no points anymore, but now our interest is in the spatial coherence between the fields at the two points at P and R. Let us consider the reciprocal process in which lights emitted from the point S propagate backward to reach the two points P and R. Remembering that the point S on the hologram is located on one of the bright fringes resulting from constructive (i.e., in phase) interference between the object and reference waves from the points P and R, we can find that the optical fields at P and R, produced by the incoherently illuminated hologram through the reciprocal process, are always in phase because the lights are emitted only from the points on the bright fringes. For example, the point sources at S and S' (on the different bright fringes) emit mutually incoherent lights, but the lights from each source arrive at the points P and R in phase, irrespective of their initial phase. As the result of superposition of many fields that are mutually in phase, the field at the point P becomes highly coherent with reference to the point R. Thus, for incoherent illumination, the on-axis hologram serves as a lens that focuses a coherence function at P axially shifted from the reference point R, while the off-axis hologram serves as a prism that shifts the high coherence point P laterally from the reference point R. Because of their functional analogies, they are called as coherence holography, a coherence lens, and a coherence prism, respectively. In the explanation above, we assumed a point source as an object, but the principle applies to a more general 3-D object composed of many point sources.

Just as a conventional computer-generated hologram (CGH) can create an arbitrary 3-D optical field, a computer-generated coherence hologram (CGCH) can synthesize an optical field with a desired 3-D coherence function between the movable observation point P and the fixed reference point R. Furthermore, the space-time symmetry in the wave equation for the coherence function in Eq. (2) indicates that the role of a temporal coherence function can be replaced by a spatial coherence function. This leads to a new principle of optical metrology that makes use of a spatial (rather than temporal) coherence function of quasi-monochromatic (rather than broadband) light synthesized by CGCH.

5.3 Analogy between temporal coherence and spatial coherence in 3-D profilometry

To see analogy between temporal coherence and spatial coherence in optical metrology, we compare techniques for 3-D profilometry. Shown in Fig. 5 (a) is a traditional white-light interferometer that makes use of short temporal coherence of

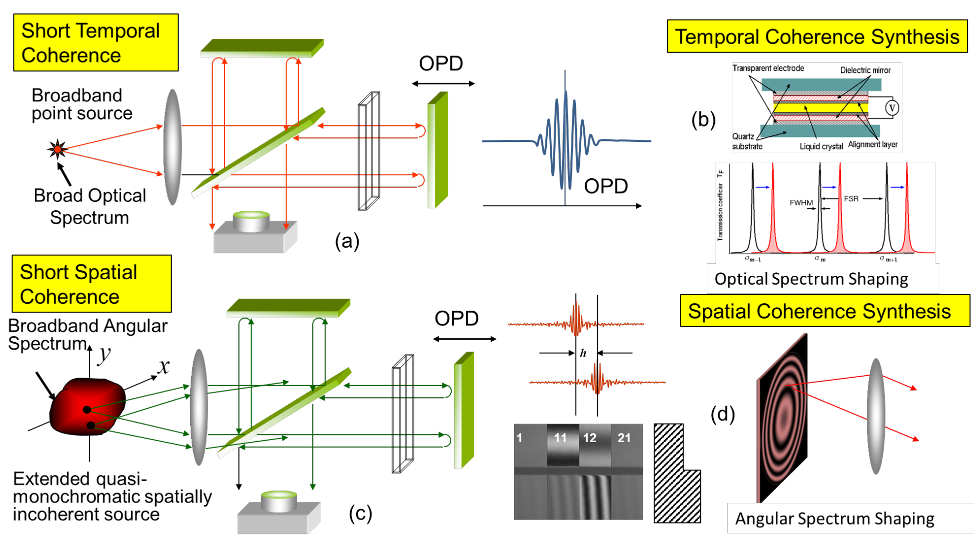

Figure 5. Temporal coherence vs. spatial coherence in 3-D profilometry. (a) Use of short temporal coherence. (b) Use of synthesized temporal coherence. (c) Use of short spatial coherence. (d) Use of synthesized spatial coherence.

the light from a broadband point source. This technique needs to scan one of the interferometer arms mechanically to find the position of zero OPD (optical path difference). This problem is solved by the technique of temporal coherence synthesis. As shown in Fig. 5 (b), a temporal coherence function is synthesized by spectrum shaping with a tunable frequency laser in such a manner that the high coherence peak is created at the desired depth position to be probed[15]. As a spatial analogue of the white-light interferometer based on temporal short coherence, we can think of the scheme shown in Fig. 5 (c), which makes use of spatial short coherence of an extended quasi-monochromatic spatially incoherent source[16]. It should be noted that quasi-monochromatic light can have short axial coherence if it has broadband angular (spatial frequency) spectra, as shown in the picture of fringes on a step height (see, the inset). Thus, the use of spatial coherence permits depth sensing (e.g., OCT) that is free from the refractive-index dispersion problem arising from the medium and/or object. As has been shown in Subsection 5.2, the axial spatial coherence function can be synthesized by angular spectrum shaping with an on-axis computer generated coherence hologram, as shown in Fig. 5 (d). The system serves as a coherence lens that focuses the spatial coherence function at the desired depth location.

5.4 3-D profilometry with synthesized spatial coherence function: An example

Among the four schemes of coherence-based 3-D profilometry shown in Fig. 5, the reader may be least familiar with the scheme that uses a synthesized spatial coherence function. To give an idea about how it works, we show a specific example[17,18] with a brief explanation. Shown in Fig. 6 (a) is an experimental setup in which light from a laser is expanded and collimated to illuminate a spatial light modulator (SLM), on which an on-axis hologram with the form of a Fresnel zone plate (FZT) is displayed. The FZT displayed on the SLM is imaged by a telecentric optical system onto a

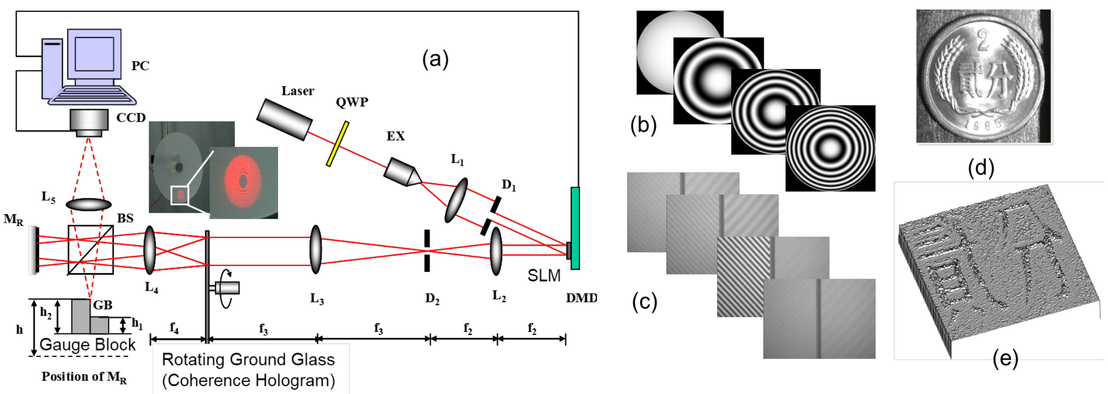

Figure 6. (a) Experimental setup. (b) Computer-generated coherence hologram for axial spatial coherence synthesis. (c) Variation of fringe contrast on a gauge block by spatial coherence focusing. (d) and (d) Object and its profile obtained. [After Z. Duan, P. Pavlicek, Y. Miyamoto, and M. Takeda, Proc. SPIE (2004).]

rotating ground glass GG, which destroys spatial coherence to create an axial coherence hologram on its surface. The light from each point source on the incoherently illuminated hologram is collimated by lens L4 to exclude a radial shear caused by beam propagation, so that the subsequent interferometer introduces only axial shear (or axial optical path difference) for sensing axial coherence. The interferometer is composed of a beam splitter BS, a reference mirror MR, and an object GB made of a pair of gauge blocks with different heights h1=1.6mm and h2=2.0mm. Lens L5 images the interference fringe pattern on the object surface onto CCD. Shown in Fig. 6 (b) is the axial coherence holograms with their focal length varied by changing the number of ring fringes in the FZP. Figure 6 (c) shows a set of interference fringes observed on the surfaces of the two block gages as the focal length of the axial coherence hologram is varied. The gauge blocks used in this example have polished surfaces, but the technique is applicable also to an object with an unpolished surface. Shown in Fig. 6 (d) and (e) are, respectively, a 2-Fen Chinese coin with an unpolished surface used as a sample, and the result of surface profilometry by axial coherence holography.

6. HOW I LEARNED FROM JIM WYANT IN THE PLAYGROUND OF OPTICAL METROLOGY

In previous sections, we have seen some of examples of the space-time analogy between the variables $\boldsymbol{r} \Leftrightarrow t$ and $\boldsymbol{k} \Leftrightarrow \omega$, as well as the signal-frequency duality between the variables $\boldsymbol{r} \Leftrightarrow \boldsymbol{k}$ and $t \Leftrightarrow \omega$ in optical metrology. As mentioned, the possible combinations of these four variables ($\boldsymbol{k}, \boldsymbol{r}; \omega, t$) in parameter space create a technological

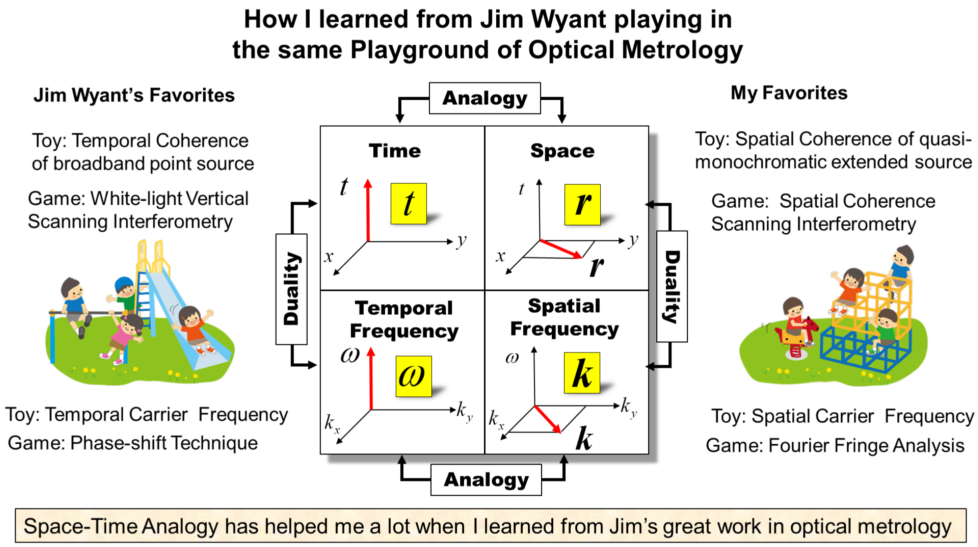

Figure 7. Playground of Optical Metrology

playground for researchers to play various games of optical metrology. As my tribute to Jim Wyant and his achievements in optical metrology, I would like to devote this final section to a description on how I learned from Jim Wyant when playing in the same playground of optical metrology. As shown in Fig. 7, the playground is composed of four play areas of quadrants with their symbols t , $\boldsymbol{r}$, ω and $\boldsymbol{k}$, and children have their favorite toys and play areas. According to my observations, one of Jim's favorite toys is short temporal coherence of a broadband source. With this toy, he enjoyed the game of white-light interferometry and made a great success[19,20]. Another toy of his favorite is temporal carrier frequency. With this toy, he enjoyed the game of the phase-shift interferometry, and gave a large impact to optical metrology[21]. To introduce myself, one of my favorite toys is spatial coherence of a quasi-monochromatic extended source. With this toy, I enjoyed the game of spatial coherence scanning interferometry together with a small number of people who love something strange. Another toy of my favorite is spatial carrier frequency, with which I enjoyed the game of Fourier fringe analysis[22]. In this way, I played mostly with spatial parameters in the ($\boldsymbol{r}$, $\boldsymbol{k}$) areas of the playground, and Jim played mostly with temporal parameters in the (t,ω) areas of the playground (though he is now enjoying the spatial parallelism of phase shifting with a polarization sensitive image sensor for his powerful toy[23]). Despite the difference of the playing areas in the playground, I learned a lot from Jim Wyant and received his great stimulus. How was it possible? It was the space-time analogy that made it possible.

I would like to take this opportunity to thank Jim for the great stimuli that he gave me for a long time, probably without noticing it himself.

REFERENCES

[1] Wyant, J. C, "Computerized interferometric surface measurements [Invited]," Appl. Opt. 52(1), 1-8 (2013).

[2] Takeda, M., "The philosophy of fringes - Analogies and dualities in fringe generation and analysis," Proc. 3rd Int. Workshop on Automatic Processing of Fringe Patterns, W. Jüptner, W. Osten Eds., [Fringe '97], Akadmie Verlag, 17-26 (1997).

[3] Massie, N. A., Nelson, R. D. and Holly, S., "High-performance real-time heterodyne interferometry," Appl. Opt. **18** (11), 1797-1803 (1979).

[4] Bruning, J. H., Herriott, D. R., Gallagher, J. E., Rosenfeld, D. P., White, A. D., and Brangaccio, D. J., "Digital wavefront measuring interferometer for testing optical surfaces and lenses," App. Opt. **13** (11), 2693-2703 (1974).

[5] Takeda, M., Ina, H. and Kobayashi, S., "Fourier-transform method of fringe-pattern analysis for computer-based topography and interferometry," J. Opt. Soc. Am. **72** (1), 156-160 (1982).

[6] Takeda, M., "Spatial-carrier fringe-pattern analysis and its applications to precision interferometry and profilometry: An overview," Industrial Metrology **1** (2), 79-99 (1990).
[7] Flourny, P.A., McClure, R. W., and Wyntjes, G., "White-light interferometric thickness gauge," Appl. Opt. **11** (9), 1907-1915 (1972).
[8] Tanaka, N., Takeda, M., and Matsumoto, K., "Interferometrically measuring the physical properties of test object," United States Patent 4,072,422 (filed October 20 1976, issued February 7, 1978).
[9] Vienot, J. C., Ferriere, R., and Goedgebur, J. P. "Conjugation of space and time variables in optics," [No. 65 of AIP Conference Proceedings of Optics in Four Dimensions], M. A. Machado and L. M. Narducci, eds. American Institute of Physics, New York, 49–62 (1981).
[10] Kim, J. A., Kim, J. W., Kang, C. S., Jin, J., and Lee, J. Y., "An interferometric system for measuring thickness of parallel glass plates without 2π ambiguity using phase analysis of quadrature Haidinger fringes," Rev. Sci. Instr. **88**, 055108 (2017).
[11] Goodman, J. W., [Statistical Optics], John Wiley & Sons, New Jersey, 193-194 (2015).
[12] Wolf, E., [Introduction to the Theory of Coherence and Polarization of Light], Cambridge Univ. Press, Cambridge, 41.
[13] Takeda, M, Wang, W., Duan, Z. and Miyamoto, Y., "Coherence holography," Opt. Express **13** (23), 9629-9635 (2005).
[14] Takeda, M., Wang, W., and Naik, D. N., "Coherence holography and photon-correlation holography: Marriage between holography and statistical optics," Proc. SPIE 8122, 812207 (2011).
[15] Hotate, K. and Okugawa, T., "Selective extraction of a two-dimensional optical image by synthesis of the coherence function," Opt. Lett. **17** (21), 1529-1531 (1992).
[16] Pavliček, P. and Takeda, M., "Similarities and differences between spatial coherence profilometry and white-light Interferometry," AIP Conference Proceedings 1236, 161 (2010).
[17] Duan, Z., Miyamoto, Y. and Takeda, M., "Dispersion-free optical coherence depth sensing with a spatial frequency comb generated by an angular spectrum modulator," Opti. Express **14** (25), 12109-12121 (2006).
[18] Duan, Z., Pavlicek, P. Miyamoto, Y., and Takeda, M., "LCD-based low spatial coherence interferometer," Proc. SPIE 5636, Holography, Diffractive Optics, and Applications II, (7 February 2005).
[19] Wyant, J. C., "White light interferometry", Proc. SPIE 4737, Holography: A Tribute to Yuri Denisyuk and Emmett Leith, (9 July 2002).
[20] Schmit, J., Creath, K., and Wyant, J. C., "Surface profilers, multiple wavelength, and white light interferometry," [Optical Shop Testing], Third Edition, D. Malacara Ed., John Wiley & Sons, 674-763 (2007).
[21] Wyant, J. C., "Phase-shifting interferometry," https://wp.optics.arizona.edu/jcwyant/published-papers/phase-shifting-interferometry/.
[22] Takeda, M., "Fourier fringe analysis and its application to metrology of extreme physical phenomena: a review [Invited]," Appl. Opt. **52** (1), 20-29 (2013).
[23] Novak, M., Millerd, J., Brock, N., North-Morris, M., Hayes, J., and Wyant, J., "Analysis of a micropolarizer array-based simultaneous phase-shifting interferometer," Appl. Opt. 44 (32) 6861-6868 (2005).